

Figure S1

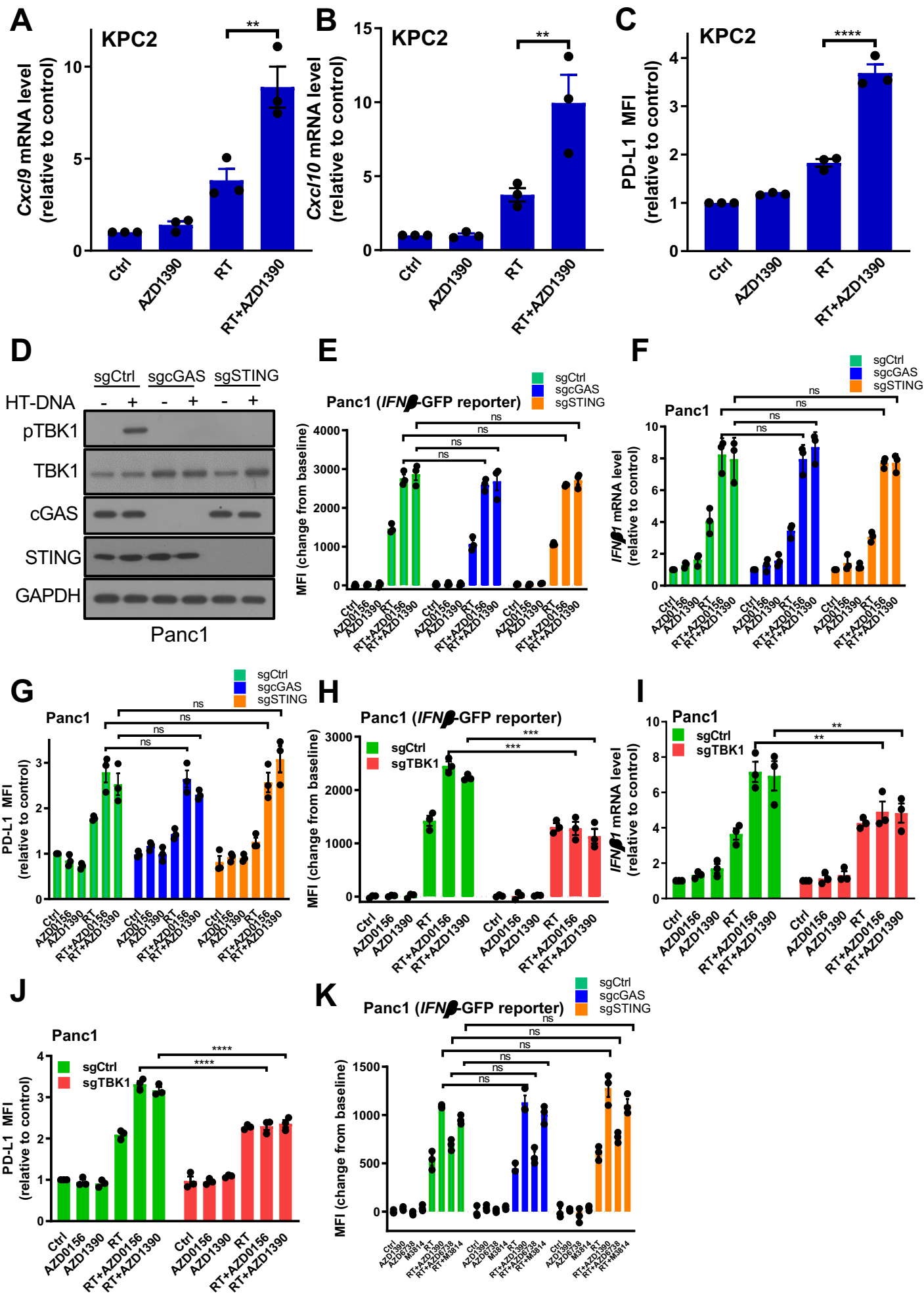
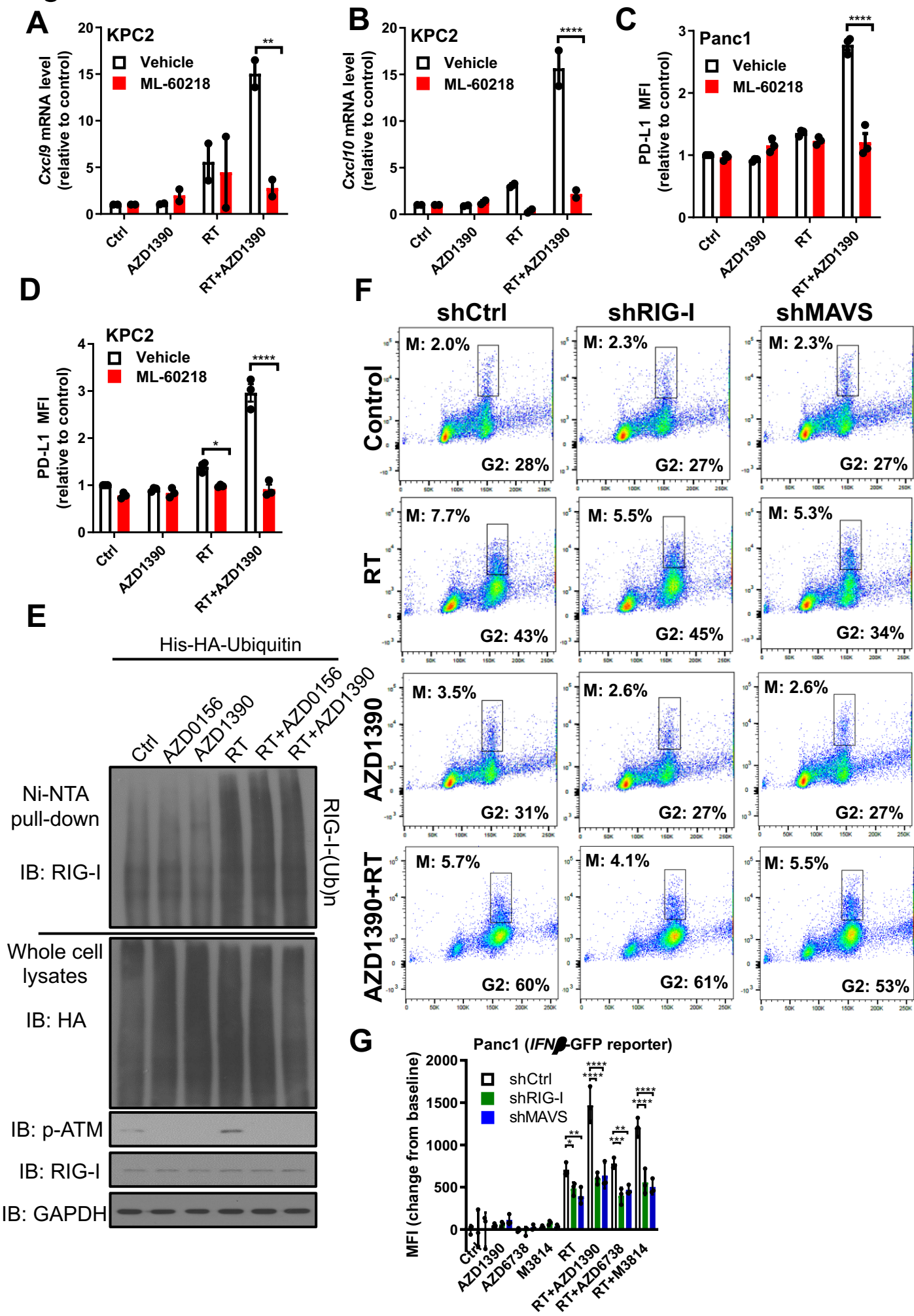
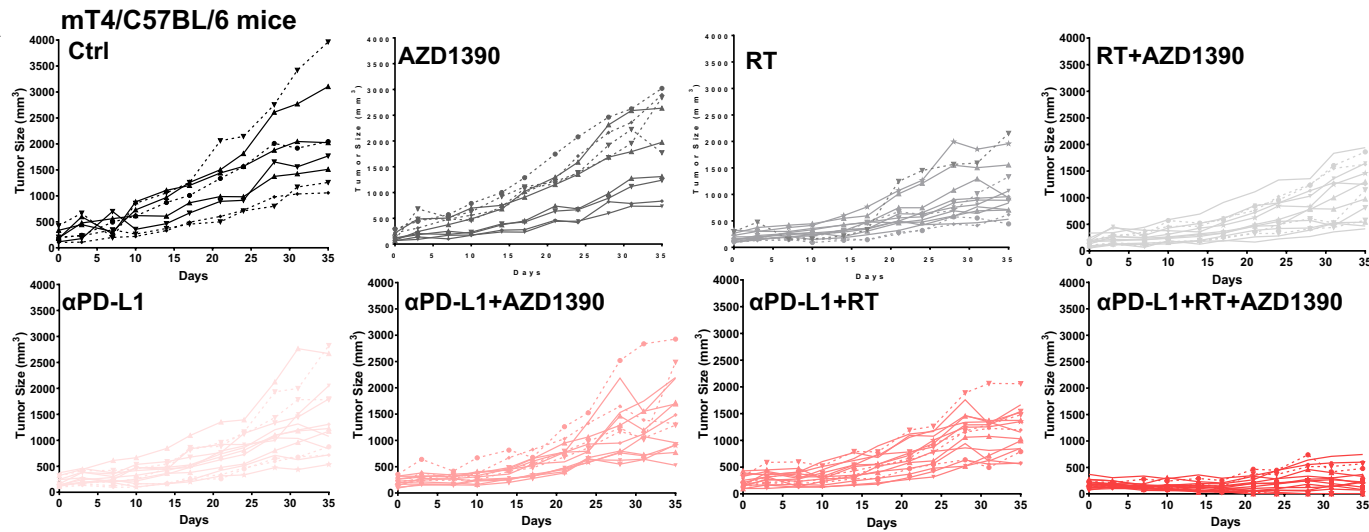


Figure S2

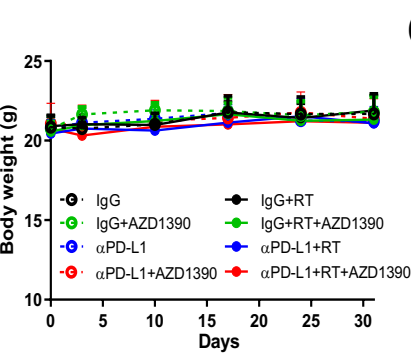


# Figure S3

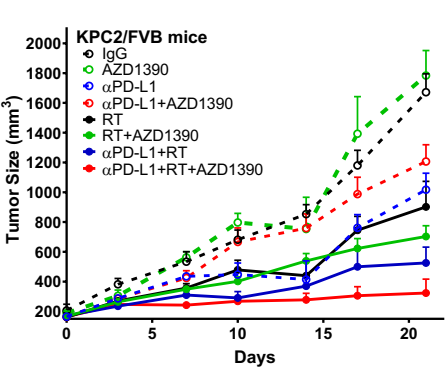
**A**



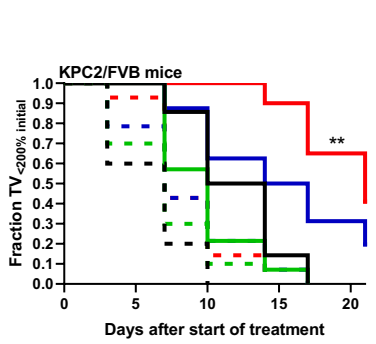
**B**



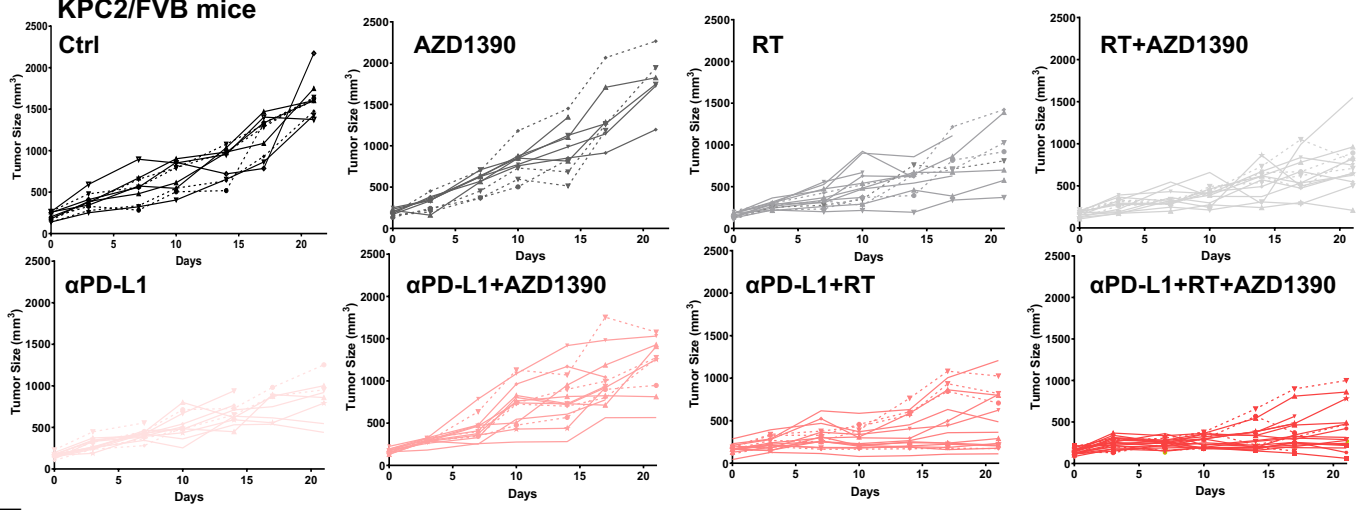
**C**



**D**



**E**



**F**

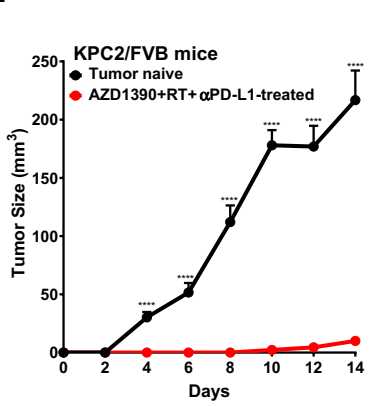
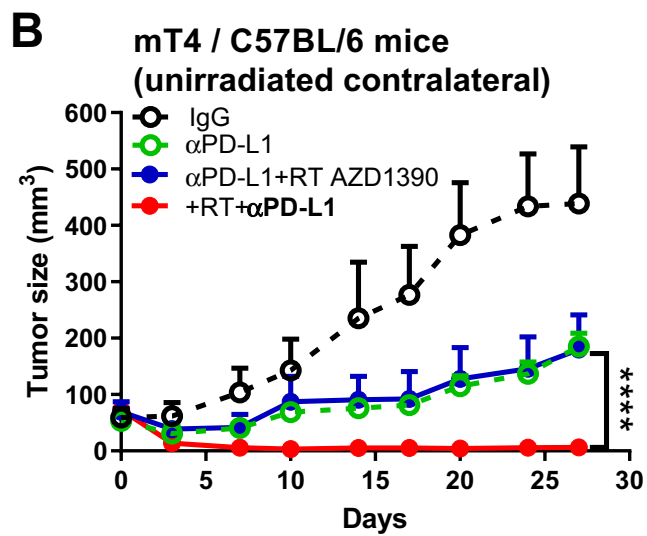
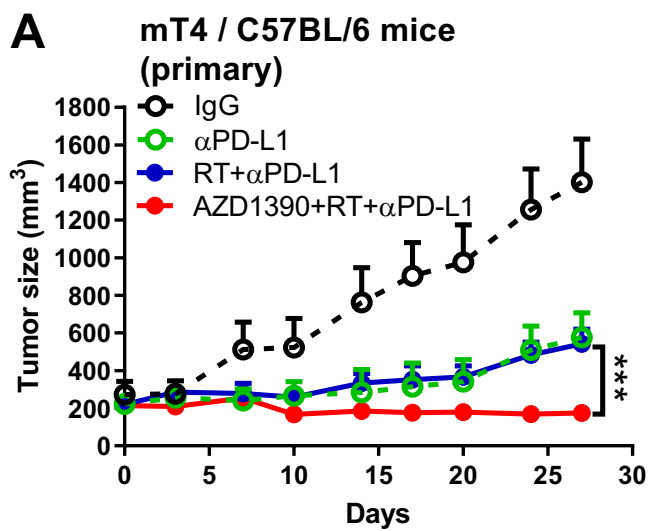






Figure S6



## Supplementary Figure Legends

**Figure S1. ATM inhibitor enhances radiation-induced T1IFN expression and signaling in a TBK1-dependent and cGAS/STING-independent manner. (A, B)** qPCR analysis of *Cxcl9* (A) and *Cxcl10* (B) mRNA levels in murine KPC2 cells at 3 days after treatment with radiation (8 Gy) and/or treatment AZD0156 (30 nM) or AZD1390 (30 nM). **(C)** Flow cytometry analysis of cell surface PD-L1 expression in KPC2 cells with the indicated treatments. Data are the MFI for PD-L1 minus the MFI for isotype control and shown as relative fold change. **(D)** Immunoblot analysis of TBK1 phosphorylation levels in Ctrl, cGAS, and STING-deleted Panc1 cells following herring testis (HT)-DNA transfection (1  $\mu$ g/ml, 4 hr). **(E)** GFP MFI in indicated (sgCtrl, sgSTING, or sgcGAS) Panc1-*IFN $\beta$ 1* promoter-GFP reporter cells at 3 days following radiation (8 Gy) and/or AZD0156 (30 nM) or AZD1390 (30 nM). **(F)** qPCR for *IFN $\beta$ 1* in indicated (sgCtrl, sgSTING, or sgcGAS) Panc1 cells 3 days after treatment with radiation (8 Gy) and/or AZD0156 (30 nM) or AZD1390 (30 nM). **(G)** Cell surface PD-L1 in Panc1 cells (sgCtrl, sgSTING, or sgcGAS) at 3 days following treatment with and/or radiation (8 Gy) and AZD0156 (30 nM) or AZD1390 (30 nM) 1hr before radiation. Data are the MFI for PD-L1 minus the MFI for isotype control and shown as relative fold change. **(H)** Ctrl and TBK1-KO *IFN $\beta$ 1* promoter-GFP reporter Panc1 cells treated with radiation (8 Gy) and/or AZD0156 (30 nM) or AZD1390 (30 nM) and tested MFI of GFP expression at Day 3. **(I)** qPCR analysis of *IFN $\beta$ 1* mRNA levels in Ctrl and TBK1-KO Panc1 cells treated with radiation (8 Gy) and/or AZD0156 (30 nM) or AZD1390 (30 nM) at Day 3. **(J)** Flow cytometry analysis of cell surface PD-L1 in Panc1 cells (sgCtrl, sgTBK1) at 3 days following treatment with radiation (8 Gy) and/or AZD0156 (30 nM) or AZD1390 (30 nM). **(K)** Ctrl, cGAS, and STING knockout Panc1 cells with stable *IFN $\beta$ 1* promoter-GFP reporter treated with radiation (8 Gy) and/or AZD1390 (30 nM), AZD6738 (200 nM), or M3814 (100 nM) and tested MFI of GFP expression at Day 3. In plots A-C and E-K, data are the mean  $\pm$  SEM (n=3 independent experiments with each performed in technical triplicate). Statistical analyses were carried out by

one-way ANOVA with a multiple comparison post-test; \*P < 0.05, \*\*P < 0.01, \*\*\*P < 0.001, \*\*\*\*P < 0.0001.

**Figure S2. Inhibition of RNA POLIII or depletion of RIG-I and MAVS blocks ATM inhibitor and radiation-induced interferon stimulated gene expression.** (A, B) *Cxcl9* and *Cxcl10* mRNA levels were measured by qPCR in KPC2 cells treated with radiation (8 Gy) and/or AZD1390 (30 nM) in the absence or presence of the POLIII inhibitor ML-60218. (C, D) Ctrl and ML-60218 treated Panc1 (C) and KPC2 (D) cells following treatment with radiation (8 Gy) and/or AZD1390 (30 nM) were analyzed for cell surface PD-L1 expression by flow cytometry. (E) His-HA-ubiquitin transfected Panc1 cells were treated with radiation (8 Gy) and/or AZD0156 (30 nM) or AZD1390 (30 nM) for 6 hours. Ubiquitination assay was performed to determine endogenous RIG-I ubiquitination using Ni-NTA beads and Western blot analysis. (F) Representative cell cycle analysis of shCtrl, shRIG-I, and shMAVS Panc1 cells at 24 hours following radiation (8 Gy) and/or AZD1390 (30 nM) with staining for DNA content (PI, x-axis) and phosphorylated-Histone H3 (Ser10; y-axis). (G) Ctrl, cGAS, and STING knockdown Panc1 cells with stable *IFNβ1* promoter-GFP reporter treated with radiation (8 Gy) and/or AZD1390 (30 nM), AZD6738 (200 nM), or M3814 (100 nM) and tested MFI of GFP expression at day 3. Data are the mean ± SEM with 2-3 independent experiments with each performed in technical triplicate. Statistical analyses were carried out by one-way ANOVA with a multiple comparison post-test; \*P < 0.05, \*\*P < 0.01, \*\*\*P < 0.001, \*\*\*\*P < 0.0001.

**Figure S3. Combined therapy with ATM inhibitor, radiotherapy, and anti-PD-L1 inhibits pancreatic tumor growth and induces durable anti-tumor immune responses.** (A) Individual tumor volumes for data shown in Figure 3B. Number of mice per (treatment arm) = 8 (ctrl), 10 (AZD1390), 14 (RT), 16 (AZD1390+RT), 12 (αPD-L1), 16 (αPD-L1+AZD1390), 16 (αPD-L1+RT), and 20 (αPD-L1+AZD1390+RT). (B) Body weight of the mice shown in Figure 3B. (C, D) FVB mice with KPC2 tumors were treated as illustrated (Figure 3A). Data are the mean tumor volume

± SEM (B) or tumor volume doubling time (C). Data are from n = 10 (ctrl), 10 (AZD1390), 12 (αPD-L1), 16 (AZD1390+αPD-L1), 14 (RT), 16 (AZD1390+RT), 16 (αPD-L1+RT), and 20 (AZD1390+RT αPD-L1) tumors per treatment group. (E) Individual tumor volumes for data shown in Figure S3C. (F) Mice with complete responses to AZD1390, RT, and αPD-L1 were rechallenged with KPC2 (10<sup>6</sup>) cells 7 days after complete response. Naïve FVB mice were similarly rechallenged. Data are the mean tumor volume from naïve (n = 10) or previously treated FVB (n=4). In Panel B, C, and F, data are the mean ± SEM. Statistical analyses were carried out by one-way ANOVA with a multiple comparison post-test; \*\*P < 0.01, \*\*\*\*P < 0.0001.

**Figure S4. ATM inhibitor, radiotherapy, and anti-PD-L1 treatment alters the tumor immune microenvironment.** (A) Cell specific markers used to identify clusters of cells from harvested subcutaneous mT4 tumors. (B) Interferon stimulated gene expression in AZD1390, RT+αPD-L1, or AZD1390+RT+αPD-L1 treatments compared to control. (C) Identification of *Cd8a* expressing cells from the T cell cluster that were used to subset and re-cluster. (D) CD8<sup>+</sup> T cell specific markers used to identify clusters. (E) GSEA plot of interferon alpha and gamma responses, and allograft rejection based on gene expression in T cells from combined therapy with radiation and anti-PD-L1. (F) GSEA normalized Hallmark pathways associated with AZD1390/RT/αPD-L1 treatment in CD8<sup>+</sup> T cells. Statistical significance in E was determined using an unpaired t-test. P value indicated.

**Figure S5. AZD1390, radiation, and αPD-L1 increase tumor-infiltrated CD8<sup>+</sup> T, but not CD4<sup>+</sup> T cell numbers.** (A) Gating strategy to determine CD90<sup>+</sup>, CD4<sup>+</sup>, and CD8<sup>+</sup> cells in the mT4 tumors treated with AZD1390, radiation, and/or αPD-L1 (as illustrated in Fig 3A) at day 10. (B) Quantitation of the percentage of tumor infiltrating lymphocyte CD4<sup>+</sup> (in the CD90<sup>+</sup> cell population) and CD8<sup>+</sup> cell numbers (in the CD90<sup>+</sup> and total cell population respectively) stained at day 10. Data are the mean ± SEM. (C) Flow cytometry for the percentage of PD1<sup>+</sup>, Tim3<sup>+</sup> positive tumor CD8<sup>+</sup> cells in mT4 tumors treated with AZD1390, radiation, and/or αPD-L1 (as illustrated in Fig

3A) and harvested at day 10. Statistical analyses were carried out by one-way ANOVA with a multiple comparison post-test; \*P < 0.05, \*\*P < 0.01, \*\*\*\*P < 0.0001.

**Figure S6. ATM inhibition, radiotherapy and  $\alpha$ PD-L1 exhibit systemic tumor control. (A, B)**

Tumor growth curves of primary tumors (A) and unirradiated contralateral tumors (B) in mT4 tumor-bearing mice after the indicated treatments. Number of mice per (treatment arm) = 5 (ctrl), 7 ( $\alpha$ PD-L1), 8 ( $\alpha$ PD-L1+RT), and 10 ( $\alpha$ PD-L1+AZD1390+RT). Data are the mean tumor volume  $\pm$  SEM. Statistical analyses were carried out by one-way ANOVA with a multiple comparison post-test; \*\*\*P < 0.001, \*\*\*\*P < 0.0001.